

OPEN ACCESS

## Bayesian uncertainty quantification applied to RANS turbulence models

To cite this article: Todd A Oliver and Robert D Moser 2011 *J. Phys.: Conf. Ser.* **318** 042032

View the [article online](#) for updates and enhancements.

### You may also like

- [Bayesian uncertainty analysis compared with the application of the GUM and its supplements](#)

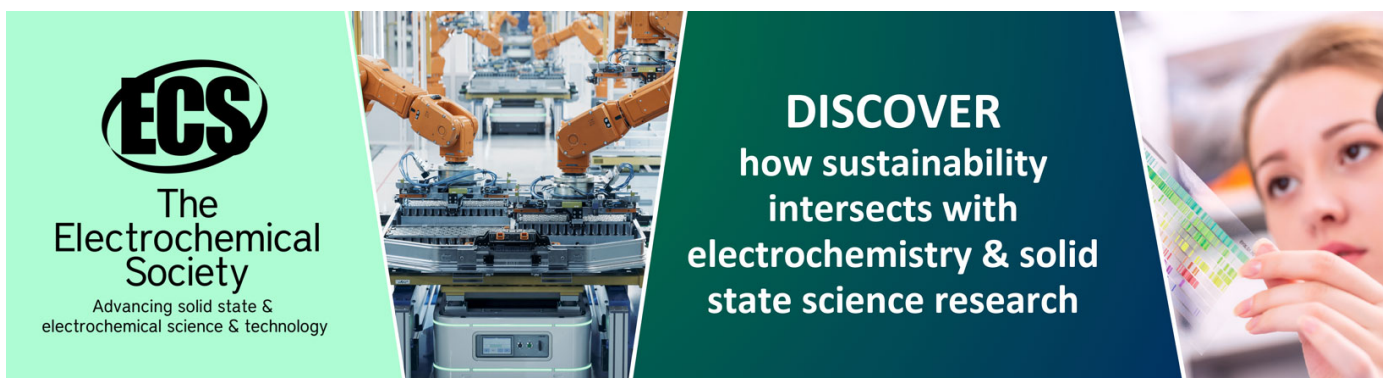
Clemens Elster

- [Spatial averaging of velocity measurements in wall-bounded turbulence: single hot-wires](#)

Jimmy Philip, Nicholas Hutchins, Jason P Monty et al.

- [Method to minimize polymer degradation in drag-reduced non-Newtonian turbulent boundary layers](#)

Lucia Baker, Yiming Qiao, Sina Ghaemi et al.



**ECS**  
The  
Electrochemical  
Society  
Advancing solid state &  
electrochemical science & technology

**DISCOVER**  
how sustainability  
intersects with  
electrochemistry & solid  
state science research

# Bayesian uncertainty quantification applied to RANS turbulence models

Todd A Oliver and Robert D Moser

Center for Predictive Engineering and Computational Sciences  
Institute for Computational Engineering and Sciences  
The University of Texas at Austin  
1 University Station, C0200, Austin, TX 78712, USA  
E-mail: [oliver@ices.utexas.edu](mailto:oliver@ices.utexas.edu)

**Abstract.** A Bayesian uncertainty quantification approach is developed and applied to RANS turbulence models of fully-developed channel flow. The approach aims to capture uncertainty due to both uncertain parameters and model inadequacy. Parameter uncertainty is represented by treating the parameters of the turbulence model as random variables. To capture model uncertainty, four stochastic extensions of four eddy viscosity turbulence models are developed. The sixteen coupled models are calibrated using DNS data according to Bayes' theorem, producing posterior probability density functions. In addition, the competing models are compared in terms of two items: posterior plausibility and predictions of a quantity of interest. The posterior plausibility indicates which model is preferred by the data according to Bayes' theorem, while the predictions allow assessment of how strongly the model differences impact the quantity of interest. Results for the channel flow case show that both the stochastic model and the turbulence model affect the predicted quantity of interest. The posterior plausibility favors an inhomogeneous stochastic model coupled with the Chien  $k$ - $\epsilon$  model. After calibration with data at  $Re_\tau = 944$  and  $Re_\tau = 2003$ , this model gives a prediction of the centerline velocity at  $Re_\tau = 5000$  with uncertainty of approximately  $\pm 4\%$ .

## 1. Introduction

In many turbulent flows of technical interest, the cost of direct numerical simulation (DNS) and large eddy simulation are prohibitive. In such cases, important design and operations decisions are informed by numerical solutions of the Reynolds-averaged Navier-Stokes (RANS) equations coupled with a closure model intended to represent the effects of turbulent fluctuations on the mean flow. However, the effects of turbulence are difficult to model, and RANS closure models are notoriously unreliable. Thus, it is important to quantify the uncertainty in RANS simulations and the effects of that uncertainty on predictions of quantities of interest (QoIs). This uncertainty quantification (UQ) process is the subject of this work.

Sources of uncertainty can be broadly divided into two classes: parameter and model. Parameter uncertainty is uncertainty that appears because the true or “best” value of a particular parameter—e.g., a closure constant in the turbulence model—is not well-known. This type of uncertainty can be treated using sensitivity analysis, interval analysis or, more generally, probabilistic analysis. In the latter, the uncertain parameters are treated as random variables and the associated joint probability density function (PDF) is propagated through the

model, leading to a PDF for the QoI. While turbulence model parameter uncertainty is widely acknowledged and has occasionally been analyzed—see, e.g., (Platteeuw *et al.*, 2008; Dunn *et al.*, 2011)—it is not standard practice in CFD analysis to attempt to quantify this uncertainty.

Model uncertainty is uncertainty that appears due model inadequacy. Model inadequacy is the inherent inability of the model to reproduce reality, even for the “best” values of the model parameters. In a prediction scenario—where experimental or high fidelity simulation (e.g., DNS) data is not available—the effect of this inadequacy on the predictions of the QoIs cannot be assessed directly via comparison with data. This fact leads to uncertainty regarding the accuracy of the prediction. While it is generally recognized that all RANS turbulence models suffer from inherent inadequacies that limit their fidelity, efforts to develop methods to systematically quantify these uncertainties have begun only fairly recently (Cheung *et al.*, 2011; Emory *et al.*, 2011; Dow & Wang, 2011).

In this work, a Bayesian probabilistic approach is used to quantify the uncertainty in predictions of RANS turbulence models. Both parameter and model uncertainty are treated. Specifically, the UQ approach involves stochastic model development, parameter calibration against data, QoI prediction, and model comparison. The approach is applied to analyze the uncertainty in mean velocity field predictions for incompressible, fully-developed channel flow. The current work represents an extension of that described by Cheung *et al.* (2011), where the Bayesian approach was applied to the calibration and validation of the Spalart-Allmaras (SA) turbulence model for boundary layer flows. Two significant extensions are achieved. First, additional turbulence models are considered, adding a dimension to the model comparison problem. Second, more complex and realistic uncertainty representations are developed, leading to improved uncertainty estimates in the predicted QoI.

The remainder of the paper is organized into four sections. The overall approach is summarized in Section 2. The specific stochastic models and calibration data used for the channel application are described in detail in Section 3, and representative results are shown in Section 4. Section 5 provides conclusions.

## 2. Bayesian Uncertainty Quantification Overview

The Bayesian UQ approach is centered around the use of probability theory to represent one’s knowledge and the use of Bayes’ theorem to update that knowledge to account for data (Jaynes, 2003; Tarantola, 2005). Thus, in contrast to typical RANS simulations where the output is a deterministic prediction, the goal of this process is to provide a PDF for the prediction QoI. To arrive at such a prediction using a typical deterministic turbulence model, three steps are required: stochastic model construction, calibration, and finally prediction. In addition, when multiple competing models (either different turbulence models or different stochastic extensions) are available, the Bayesian framework provides a natural metric, known as the posterior model plausibility, to compare the models in the light of the available data. These processes are briefly described in Sections 2.1 through 2.4.

### 2.1. Stochastic Modeling

A stochastic extension of the deterministic model of interest is required to enable the model to make stochastic predictions. The most basic stochastic extension of any deterministic model is constructed by simply viewing the model parameters as random variables. This construction captures parameter uncertainty but is unable to account for model uncertainty. In general, this approach is not sufficient for eddy viscosity-based turbulence models, where model uncertainty is expected to be significant.

Given that eddy viscosity-based models do not accurately represent the physics of the flow, it makes sense to view their predictions not as precise predictions of the mean flow but rather

as information that can be used to construct a PDF over the space of possible mean flow fields. For example, one could use the following form:

$$\langle \vec{u} \rangle(\vec{x}, t; \boldsymbol{\theta}, \boldsymbol{\alpha}) = \vec{U}(\vec{x}, t; \boldsymbol{\theta}) + \vec{\epsilon}(\vec{x}, t; \boldsymbol{\alpha}). \quad (1)$$

In (1),  $\vec{U}$  denotes the mean flow velocity given by the RANS model, which is a function of spatial location  $\vec{x}$ , time  $t$ , and turbulence model parameters  $\boldsymbol{\theta}$ ;  $\vec{\epsilon}$  is a random vector field that may depend on additional parameters  $\boldsymbol{\alpha}$ ; and  $\langle \vec{u} \rangle$  denotes the stochastic prediction of the true mean velocity field. Here,  $\vec{\epsilon}$  represents uncertainty introduced by the RANS model inadequacy. Of course, the actual mean velocity is not random. Thus, the fact that  $\langle \vec{u} \rangle$  is random reflects incomplete knowledge of the true mean velocity. To complete the model, one must precisely define the random field  $\vec{\epsilon}$ . Section 3.2 gives a complete description of the stochastic models developed in this work.

## 2.2. Calibration

Calibration is the process of extracting knowledge about model parameters from data. In the current work, the goal of the calibration procedure is to inform both the turbulence model closure constants,  $\boldsymbol{\theta}$ , and any additional parameters introduced by the stochastic model extension,  $\boldsymbol{\alpha}$ .

In the Bayesian framework, the model parameters are viewed as random variables. The PDFs for these random variables represent the state of knowledge regarding their values. Thus, the solution of the calibration problem is the conditional PDF for the parameters given the calibration data. This conditional PDF is referred to as the posterior PDF and is obtained from Bayes' theorem as follows:

$$p(\boldsymbol{\theta}, \boldsymbol{\alpha} | \mathbf{d}) = k p(\boldsymbol{\theta}, \boldsymbol{\alpha}) L(\boldsymbol{\theta}, \boldsymbol{\alpha}; \mathbf{d}), \quad (2)$$

where  $\mathbf{d}$  denotes the data. Furthermore, in (2),  $p(\boldsymbol{\theta}, \boldsymbol{\alpha})$  denotes the so-called prior PDF;  $L(\boldsymbol{\theta}, \boldsymbol{\alpha}; \mathbf{d})$  denotes the likelihood function, and  $k$  is a normalization constant. The prior PDF encodes knowledge of the parameter values that is independent of the data, and the likelihood function quantifies the probability of the given data as a function of the parameter values. In particular, the likelihood function is defined by

$$L(\boldsymbol{\theta}, \boldsymbol{\alpha}; \mathbf{d}) \equiv p(\mathbf{d} | \boldsymbol{\theta}, \boldsymbol{\alpha}), \quad (3)$$

where  $p(\mathbf{d} | \boldsymbol{\theta}, \boldsymbol{\alpha})$  is the conditional PDF for the data given the parameters. For insight into the likelihood function, note that

$$p(\mathbf{d} | \boldsymbol{\theta}, \boldsymbol{\alpha}) = \int p(\mathbf{d} | \mathbf{d}_t, \boldsymbol{\theta}, \boldsymbol{\alpha}) p(\mathbf{d}_t | \boldsymbol{\theta}, \boldsymbol{\alpha}) d\mathbf{d}_t,$$

where  $\mathbf{d}_t$  denotes the unknown true data (i.e., what would be observed if the measurement process were perfect). The conditional PDF  $p(\mathbf{d} | \mathbf{d}_t, \boldsymbol{\theta}, \boldsymbol{\alpha}) = p(\mathbf{d} | \mathbf{d}_t)$  quantifies uncertainty in the measurement or observation process used to obtain the data. This PDF is constructed based on knowledge of the experiment or data set. The conditional PDF  $p(\mathbf{d}_t | \boldsymbol{\theta}, \boldsymbol{\alpha})$  represents the prediction of the true data, as given by the stochastic model discussed in Section 2.1.

## 2.3. Prediction

Although it is often computationally expensive, the prediction step is conceptually the simplest of the four tasks that make up the UQ process. After calibration, the parameter posterior PDFs are propagated through the stochastic model to compute the PDF for the QoI. The most straightforward method to accomplish this propagation is basic Monte Carlo sampling, which is used here.

#### 2.4. Model Comparison

The stochastic modeling, calibration, and prediction steps can be carried out using a single physical model with a single stochastic extension. However, it is often the case that multiple physical models of similar *a priori* fidelity are available. In this situation, it is unclear what physical model should be used for prediction. Furthermore, it is generally unclear what stochastic extension of a given physical model is most appropriate. Thus, in practice, one is confronted with multiple models that could be used for the same prediction. In the Bayesian framework, these competing models can be compared based on the posterior model plausibility.

The posterior plausibility quantifies the relative probability that a particular model in a given set produced the observed data. In particular, given a set of models  $\mathcal{M} = \{M_1, \dots, M_N\}$ , the posterior plausibility for model  $M_i$  is defined as (Jaynes, 2003; Beck & Yuen, 2004)

$$P(M_i|\mathbf{d}, \mathcal{M}) = C P(M_i|\mathcal{M}) E(M_i; \mathbf{d}, \mathcal{M}) \quad (4)$$

where  $P(M_i|\mathcal{M})$  is the prior model plausibility,  $E$  is the evidence, and  $C$  is a normalization constant. Note that the evidence plays the role of the likelihood function in (2). Specifically, it quantifies the probability of observing  $\mathbf{d}$  given  $M_i$ . Thus,

$$E(M_i; \mathbf{d}, \mathcal{M}) \equiv p(\mathbf{d}|M_i, \mathcal{M}) = \int p(\boldsymbol{\theta}, \boldsymbol{\alpha}|M_i, \mathcal{M}) p(\mathbf{d}|\boldsymbol{\theta}, \boldsymbol{\alpha}, M_i, \mathcal{M}) d\boldsymbol{\theta} d\boldsymbol{\alpha}, \quad (5)$$

which is simply the normalization constant  $k$  from Bayes' theorem (2) applied to model  $M_i$ .

### 3. Formulation Details

To exercise the framework described in Section 2, the approach is applied to the prediction of the centerline velocity in a fully-developed, incompressible channel flow at  $Re_\tau = 5000$ . Four turbulence models are coupled with four stochastic extensions to give sixteen total models that are calibrated using DNS data at two lower Reynolds numbers, compared, and used to predict the QoI. This section describes the models and the calibration data.

#### 3.1. Turbulence Models

The RANS equations for incompressible, fully-developed channel flow are well-known (Durbin & Petterson Reif, 2001) and are not repeated here. Four well-known turbulence models are used: Baldwin-Lomax (Baldwin & Lomax, 1978), SA (Spalart & Allmaras, 1994), Chien  $k-\epsilon$  (Chien, 1982), and  $v^2-f$  (Durbin, 1995; Durbin & Petterson Reif, 2001). For brevity, full details of the model equations are not given here. However, for completeness, differences between the current implementation and the references are summarized and the turbulence model calibration parameters are listed.

**3.1.1. Baldwin-Lomax** The Baldwin-Lomax (BL) model was originally formulated by Baldwin & Lomax (1978). The form of the model used here is exactly as described by Wilcox (2006). The calibration parameters are  $\kappa$ ,  $A^+$ ,  $(\alpha C_{cp})$ ,  $C_{wk}$ , and  $C_{kleb}$ . Note that  $\alpha$  (the Clauser parameter) and  $C_{cp}$  are typically viewed as two separate parameters. However, only the product appears in the BL model. Thus, the product is treated as a single parameter in this work.

**3.1.2. Spalart-Allmaras** The SA model (Spalart & Allmaras, 1994) is slightly modified from its original form to avoid undesirable behavior due to the  $f_{v2}$  closure function. This modification is originally due to Allmaras (2007) and is fully documented by Oliver & Darmofal (2009). The calibration parameters are  $c_{b1}$ ,  $c_{b2}$ ,  $\sigma$ ,  $c_{v1}$ ,  $c_{w2}$ ,  $c_{w3}$ , and  $\kappa$ .

*3.1.3. Chien  $k$ - $\epsilon$*  The Chien (1982) model is implemented exactly as described by Wilcox (2006). The calibration parameters are  $C_\mu$ ,  $C_{\epsilon 1}$ ,  $C_{\epsilon 2}$ ,  $\sigma_k$ ,  $\sigma_\epsilon$ ,  $C_{f1}$ ,  $C_{f2}$ ,  $C_{f\mu}$ . The symbols  $C_{f1}$ ,  $C_{f2}$ , and  $C_{f\mu}$  are not standard. These are closure constants appearing in the Chien closure functions as follows:

$$\nu_t = C_\mu \frac{k^2}{\epsilon} [1 - \exp(-C_{f\mu} y^+)], \quad f = 1 - C_{f1} \exp\left(C_{f2} \frac{k^2}{\nu \epsilon}\right).$$

*3.1.4.  $v^2$ - $f$*  Two changes are made from the  $v^2$ - $f$  model as specified by Durbin & Petterson Reif (2001). First, a change of variables is used to write the model in terms of  $\zeta = \overline{v'^2}/k$ . Second, the variation in  $C_{\epsilon 1}$  is neglected. Thus, the calibration parameters are  $C_\mu$ ,  $C_{\epsilon 1}$ ,  $C_{\epsilon 2}$ ,  $\sigma_\epsilon$ ,  $C_L$ ,  $C_\eta$ ,  $C_T$ ,  $c_1$ , and  $c_2$ . The notation  $C_T$  is not standard. Here,  $C_T$  refers to the closure constant in the time scale function (Durbin, 1991):

$$T = \max\left(\frac{k}{\epsilon}, C_T \sqrt{\frac{\nu}{\epsilon}}\right).$$

### 3.2. Uncertainty Models

Four competing stochastic extensions of the eddy viscosity turbulence models are developed. Each stochastic extension is appropriate for use with each turbulence model, leading to sixteen total combinations. The first three stochastic extensions are developed in terms of the mean velocity, which is both the observable used for the calibration and the QoI. While this approach is sufficient here, it is not general enough for more complex cases. In particular, since the full Reynolds stress tensor cannot be computed given only the mean velocity field, a mean velocity uncertainty model is insufficient if the Reynolds stress is the calibration observable or the prediction QoI. Thus, an additional model is constructed explicitly in terms of the Reynolds shear stress.

*3.2.1. Multiplicative Velocity Error Models* Three stochastic model extensions based on the assumption of a multiplicative error in the mean streamwise velocity are developed. All three models take the following multiplicative form:

$$\langle u \rangle^+(\eta; \boldsymbol{\theta}, \boldsymbol{\alpha}) = (1 + \epsilon(\eta; \boldsymbol{\alpha})) U^+(\eta; \boldsymbol{\theta}), \quad (6)$$

where  $\eta = y/h$  is the wall-normal coordinate non-dimensionalized by the channel half-height,  $U^+ = U/u_\tau$  is mean velocity non-dimensionalized by the friction velocity as given by RANS, and  $\langle u \rangle^+$  is the stochastic prediction of the true non-dimensionalized mean velocity. The error field,  $\epsilon$ , is chosen to be a zero-mean Gaussian random field. Thus, to complete the model, it is necessary to specify the covariance of  $\epsilon$ . Three covariance structures are examined, leading to three different stochastic models.

The first model assumes the data points are independent. Thus,

$$\langle \epsilon(\eta) \epsilon(\eta') \rangle = \sigma^2 \delta(\eta - \eta'), \quad (7)$$

where  $\delta$  is the Dirac delta distribution and  $\sigma$  is a calibration parameter. The assumption of independent errors in the mean velocity is clearly unrealistic. Thus, models with spatial correlation are necessary.

A very simple correlation can be introduced using the following homogeneous correlation structure:

$$\langle \epsilon(\eta) \epsilon(\eta') \rangle = \sigma^2 \exp\left(-\frac{1}{2} \frac{(\eta - \eta')^2}{\ell^2}\right), \quad (8)$$

where  $\sigma$  and the correlation length scale,  $\ell$ , are calibration parameters.

While it is expected that the velocity errors are correlated, a homogeneous correlation structure, as given in (8), is very restrictive and seems unlikely to be correct. Given the known structure of the channel flow, where the length scale is set by the viscous length near the wall and the channel height far from the wall, it is reasonable to expect that this multiscale structure will also appear in the error. To allow the correlation length to vary in space, the following covariance is chosen (Rasmussen & Williams, 2006):

$$\langle \epsilon(\eta)\epsilon(\eta') \rangle = \sigma^2 \left( \frac{2\ell(\eta)\ell(\eta')}{\ell^2(\eta) + \ell^2(\eta')} \right)^{1/2} \exp \left( -\frac{(\eta - \eta')^2}{\ell^2(\eta) + \ell^2(\eta')} \right), \quad (9)$$

where  $\sigma$  is a calibration parameter and  $\ell(\eta)$  is a length scale function. Specifically,

$$\ell(\eta) = \begin{cases} \ell_{in} & \text{for } \eta < \eta_{in} \\ \ell_{in} + \frac{\ell_{out} - \ell_{in}}{\eta_{out} - \eta_{in}} (\eta - \eta_{in}) & \text{for } \eta_{in} \leq \eta \leq \eta_{out} \\ \ell_{out} & \text{for } \eta > \eta_{out} \end{cases}, \quad (10)$$

where  $\ell_{in} = \ell_{in}^+ / Re_\tau$  and  $\eta_{in} = \eta_{in}^+ / Re_\tau$ . The constants  $\ell_{in}^+$ ,  $\eta_{in}^+$ ,  $\ell_{out}$  and  $\eta_{out}$  are all calibration parameters.

**3.2.2. Additive Reynolds Stress Model** The Reynolds stress uncertainty model takes the following form:

$$\langle u'v' \rangle^+(\eta; \boldsymbol{\theta}, \boldsymbol{\alpha}) = T^+(\eta; \boldsymbol{\theta}) - \epsilon(\eta; \boldsymbol{\alpha}), \quad (11)$$

where  $T^+$  is the Reynolds shear stress given by the RANS+turbulence model equations,  $\epsilon$  is a random field, and  $\langle u'v' \rangle^+$  is the stochastic prediction of the actual Reynolds shear stress.

Some clarifying remarks are necessary to understand the procedure. In particular, the stochastic mean velocity is found by solving the mean momentum equation using  $\langle u'v' \rangle^+$ :

$$-\frac{d}{d\eta} \left( \frac{1}{Re_\tau} \frac{d\langle u \rangle^+}{d\eta} - \langle u'v' \rangle^+ \right) = 1. \quad (12)$$

Note that the turbulence model is only used to define the baseline Reynolds stress,  $T^+$ , that is used to construct the stochastic Reynolds stress model. That is, the Reynolds stress PDF is only propagated through the mean momentum equation, which is not uncertain, and not through the turbulence model, which is highly uncertain. This implies that solution realizations are not required to satisfy the turbulence model. However, since it is the turbulence model that introduces the error into the system, there is no reason to require that it be satisfied.

Of course, there are infinitely many possibilities for  $\epsilon$ . To illustrate the method  $\epsilon$  is taken to be a zero-mean Gaussian random field with the following covariance:

$$\langle \epsilon(\eta)\epsilon(\eta') \rangle = k_{in}(\eta, \eta') + k_{out}(\eta, \eta'), \quad (13)$$

where  $k_{in}$  is intended to represent the near-wall error and  $k_{out}$  models the error far from the wall. The following choices are reasonable:

$$k_{in}(\eta, \eta') = \sigma_{in}^2 \left( 1 - \frac{(\eta - \eta')^2}{\ell_{in}^2} - \frac{(\eta - \eta')^2}{\Delta^2} + \frac{\ell_{in}^2}{\Delta^2} \frac{\eta\eta'}{\Delta^2} \right) \exp \left( -\frac{1}{2} \frac{(\eta - \eta')^2}{\ell_{in}^2} - \frac{1}{2} \frac{(\eta^2 + \eta'^2)}{\Delta^2} \right),$$

$$k_{out}(\eta, \eta') = \sigma_{out}^2 \left( 1 - \frac{(\eta - \eta')^2}{\ell_{out}^2} \right) \exp \left( -\frac{1}{2} \frac{(\eta - \eta')^2}{\ell_{out}^2} \right),$$

where  $\ell_{in} = \ell_{in}^+ / Re_\tau$ ,  $\Delta = C_d \ell_{in}$ , and  $\sigma_{out} = C_s / Re_\tau$ . The calibration parameters are  $\sigma_{in}$ ,  $\ell_{in}^+$ ,  $C_d$ ,  $C_s$ , and  $\ell_{out}$ .

Given this  $\epsilon$  one can analytically integrate (12) to find the random field model for the velocity.

**Table 1.** Stochastic model extension labels.

Model Description	Label	Defining Equation
Independent, homogeneous	IND	7
Correlated, homogeneous	SE	8
Correlated, inhomogeneous	VLSE	9
Additive Reynolds Stress	ARSM	11, 13

*3.2.3. Labels* Table 1 presents shorthand that will be used to refer to the stochastic models.

### *3.3. Calibration Data*

The calibration data is taken from the channel flow DNS of Jimenez and coworkers (Hoyas & Jimenez, 2006; del Alamo *et al.*, 2004). Specifically, mean velocity measurements at  $Re_\tau = 944$  and  $Re_\tau = 2003$  are used. As detailed in Section 2.2, the uncertainty in the data is incorporated in the calibration problem via the likelihood formulation. When using DNS data, the dominate uncertainty is due to the averaging process—i.e., the fact that the only a sample mean, not the true mean, is computed. An estimate of this variance, computed by the method shown by Hoyas & Jimenez (2008), is provided with the reported profile statistics. However, the covariance between points in the profile is not estimated. Thus, to minimize the impact of correlation, the profile data are downsampled such that the points are farther apart in space. After this downsampling, the DNS data points are assumed to be independent with the variance provided with the data.

## **4. Results**

This section shows a representative subset of the results obtained using the Bayesian UQ framework for the channel flow problem with the models described in Section 3. These results were generated using the Advanced Multi-Level sampling algorithm (Cheung & Beck, 2009; Cheung & Prudencio, 2011) implemented as part of the QUESO library (Prudencio & Schulz, 2011).

### *4.1. Calibration*

For each of the sixteen models defined in Section 3, the result of the calibration problem is the full joint posterior PDF defined by (2). Thus, for brevity, it is not possible to show all calibration results here. To give the flavor of the output, two example posterior PDFs are examined. Specifically, Figure 1 shows the marginal PDFs for the SA parameters  $\kappa$  and  $c_{v1}$  as well as the Chien parameters  $\sigma_k$  and  $\sigma_\epsilon$ . Both results were obtained using the VLSE model. In addition to the marginal posterior PDFs, the samples from the full joint posterior are projected onto the plane to indicate correlation between the two parameters shown. It is clear that the SA parameters ( $\kappa$  and  $c_{v1}$ ) have posterior maximizers near their nominal values (all parameters are normalized such that 1.0 is the nominal value) and are very highly correlated. Alternatively, the posterior maximizer for the Chien  $\sigma_k$  parameter is approximately 1.6 times larger than its nominal value, indicating that larger than nominal values of  $\sigma_k$  are necessary to fit the calibration data.

### *4.2. Model Comparison*

Table 2 gives  $\log(E)$ , where  $E$  is defined in (5), for each of the sixteen models defined by coupling a turbulence model with a stochastic extension. First, note that the VLSE and ARSM models

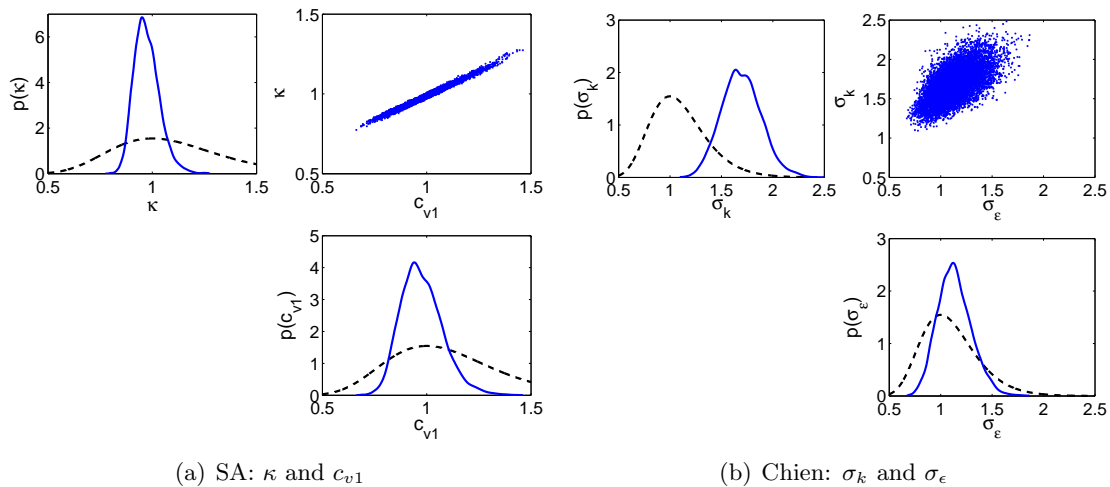


**Figure 1.** Diagonal: Marginal prior (dashed) and posterior (solid) PDFs. Upper, right: Samples projected onto plane. The parameters are normalized such that 1.0 indicates the standard value.

**Table 2.**  $\log(E)$  value for each model.

	BL	SA	Chien	$v^2-f$
IND	44.19	8.862	21.78	20.23
SE	41.71	8.045	19.94	40.45
VLSE	159.5	164.0	175.5	169.8
ARSM	135.0	169.0	157.5	158.9

have significantly larger evidence than either the IND or SE models, regardless of turbulence model. This result confirms that the inhomogeneous stochastic models are able to represent the turbulence model error better than their homogeneous competitors. Second, it is clear that a proper stochastic model extension is critical to the physical model comparison. If the inhomogeneous stochastic models had not been developed, the BL turbulence model would have the largest evidence—i.e., it would appear the most probable.

Finally, assuming a uniform prior, one can compute the posterior plausibility from the evidence. In this case, most of the models have posterior plausibility very close to zero. The model with the largest posterior plausibility is the Chien, VLSE model at 0.995. The  $v^2-f$ , VLSE and SA, ARSM models have posterior plausibility of  $3.33 \times 10^{-3}$  and  $1.50 \times 10^{-3}$ , respectively. All the other models have posterior plausibility of  $10^{-5}$  or less. Clearly, this result indicates that the calibration data strongly favors the Chien, VLSE model. However, this result does not imply that the Chien model is the “best” turbulence model in any general sense. Additional data and/or additional models could lead to different posterior plausibility results.

#### 4.3. Prediction

The centerline velocity at  $Re_\tau = 5000$  is the prediction QoI. Recall that no data at  $Re_\tau = 5000$  is used in the calibration, and no DNS data for  $Re_\tau = 5000$  is available for comparison. Figure 2 shows the PDFs for the QoI. Two sets of results are shown. Figure 2(a) shows the QoI PDF given by the Chien turbulence model coupled with each stochastic extension. The stochastic model affects both the predicted mean and uncertainty. Most notably, the IND and SE models

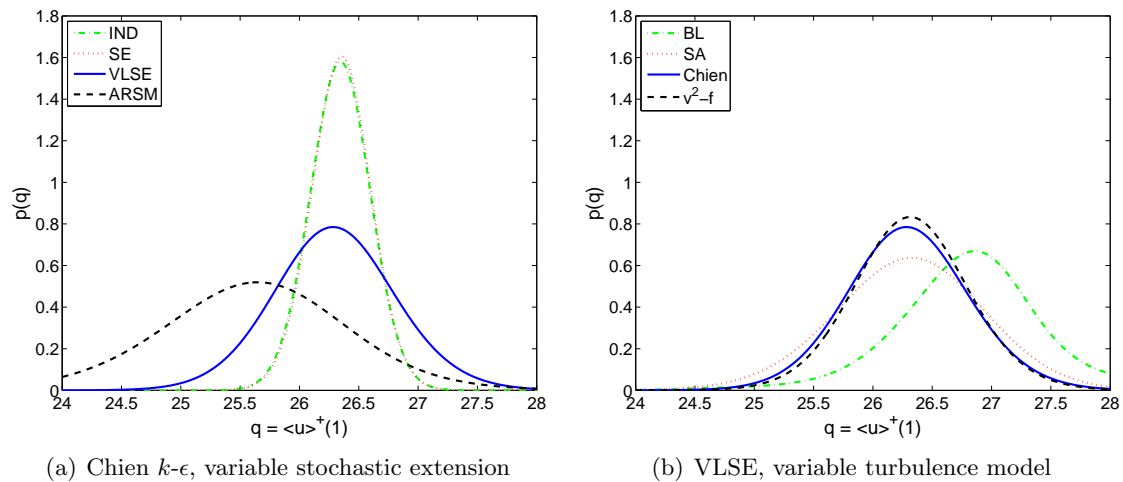


**Figure 2.** PDFs for the QoI. Left: The Chien  $k-\epsilon$  turbulence model coupled with each stochastic extension. Right: Each turbulence model coupled with the VLSE stochastic extension.

give significantly smaller uncertainty than the VLSE model. However, the evidence deems them extremely unlikely given the data. Thus, one cannot trust their predictions.

Figure 2(b) compares results generated by the different turbulence models using the VLSE stochastic extension. The Chien and  $v^2-f$  models agree quite closely. The SA model gives nearly the same mean but slightly larger uncertainty. Only the BL model appears to give significantly different results.

## 5. Conclusions

A Bayesian approach has been developed and applied to quantify uncertainty in RANS turbulence models. The approach consists of four stages: stochastic model development, calibration, model comparison, and prediction. These stages lead to a probabilistic prediction of the QoI that accounts for both parameter and model uncertainty.

The UQ procedure was applied to incompressible, fully-developed channel flow. The evidence strongly supports the use of inhomogeneous stochastic models, and the Chien  $k-\epsilon$  model was found to have the highest posterior plausibility. Using this model, the centerline velocity at  $Re_\tau = 5000$  is predicted with an uncertainty of approximately  $\pm 4\%$ .

Ongoing work is focused on developing new stochastic extensions, particularly stochastic models for the Reynolds stress tensor, for application in more complex flows.

## Acknowledgments

This material is based upon work supported by the United States Department of Energy [National Nuclear Security Administration] under Award Number [DE-FC52-08NA28615]. The authors would like to thank Profs. J. Jimenez and R. D. Moser and Drs. J.-C. del Alamo and P. S. Zandonade for generating and providing the DNS data used in this study.

## References

- DEL ALAMO, J.-C., JIMENEZ, J., ZANDONADE, P. & MOSER, R. D. 2004 Scaling of the energy spectra of turbulent channels. *J. Fluid Mech.* **500**, 135–144.

- ALLMARAS, S. R. 2007 Personal Communication via email with T. Oliver.
- BALDWIN, B. S. & LOMAX, H. 1978 Thin-layer approximation and algebraic model for separated turbulent flows. *AIAA Paper 78-257*.
- BECK, J. L. & YUEN, K. V. 2004 Model selection using response measurements: Bayesian probabilistic approach. *J. Eng. Mech.* **130**, 192–203.
- CHEUNG, S. H. & BECK, J. L. 2009 New bayesian updating methodology for model validation and robust predictions of a target system based on hierarchical subsystem tests. *Computer Methods in Applied Mechanics and Engineering*. Accepted for publication.
- CHEUNG, S. H., OLIVER, T. A., PRUDENCIO, E. E., PRUDHOMME, S. & MOSER, R. D. 2011 Bayesian uncertainty analysis with applications to turbulence modeling. *Reliab. Eng. Syst. Safety*.
- CHEUNG, S.-H. & PRUDENCIO, E. E. 2011 Parallel multi level algorithms for sampling multimodal distributions. In preparation.
- CHIEN, K.-Y. 1982 Predictions of channel and boundary-layer flows with a low-Reynolds-number turbulence model. *AIAA J.* **20** (1), 33–38.
- DOW, E. & WANG, Q. 2011 Quantification of structural uncertainties in the  $k$ - $\omega$  turbulence model. *AIAA Paper 2011-1762*.
- DUNN, M. C., SHOTORBAN, B. & FRENDI, A. 2011 Uncertainty quantification of turbulence model coefficients via Latin Hypercube Sampling method. *J. Fluids Eng.* **33** (4).
- DURBIN, P. A. 1991 Near-wall turbulence closure modeling without damping functions. *Theor. Comp. Fluid Dyn.* **3** (1), 1–13.
- DURBIN, P. A. 1995 Separated flow computations with the  $k$ - $\epsilon$ - $v^2$  model. *AIAA J.* **33** (4), 659–664.
- DURBIN, P. A. & PETTERSON REIF, B. A. 2001 *Statistical Theory and Modeling for Turbulent Flows*. Wiley.
- EMORY, M., PECNIK, R. & IACCARINO, G. 2011 Modeling structural uncertainties in Reynolds-averaged computations of shock/boundary layer interactions. *AIAA Paper 2011-479*.
- HOYAS, S. & JIMENEZ, J. 2006 Scaling of velocity fluctuations in turbulent channels up to  $Re_\tau = 2003$ . *Phys. of Fluids* **18** (011702).
- HOYAS, S. & JIMENEZ, J. 2008 Reynolds number effects on the Reynolds-stress budgets in turbulent channels. *Phys. of Fluids* **20** (101511).
- JAYNES, E. T. 2003 *Probability Theory: The Logic of Science*. Cambridge University Press.
- OLIVER, T. A. & DARMOFAL, D. L. 2009 Impact of turbulence model irregularity on high-order discretizations. *AIAA Paper 2009-953*.
- PLATTEEUW, P. D. A., LOEVEN, G. J. A. & BIJL, H. 2008 Uncertainty quantification applied to the  $k$ - $\epsilon$  model of turbulence using the probabilistic collocation method. *AIAA Paper 2008-2150*.
- PRUDENCIO, E. E. & SCHULZ, KARL W. 2011 The parallel c++ statistical library ‘QUESO’: Quantification of uncertainty for estimation, simulation and optimization. Submitted.
- RASMUSSEN, C. E. & WILLIAMS, C. K. I. 2006 *Gaussian Processes for Machine Learning*. MIT Press.
- SPALART, P. R. & ALLMARAS, S. R. 1994 A one-equation turbulence model for aerodynamic flows. *La Recherche Aéronautique* **1**, 5–32, (See also AIAA Paper 92-439).
- TARANTOLA, A. 2005 *Inverse Problem Theory and Methods for Model Parameter Estimation*. SIAM.
- WILCOX, D. C. 2006 *Turbulence Modeling for CFD*. DCW Industries, Inc.